NASA-TM-79177 19790018145

DOE/NASA/1044-79/2
NASA TM-79177

PERFORMANCE OF A 14.9-kW LAMINATED-FRAME DC SERIES MOTOR WITH CHOPPER CONTROLLER

John R. Schwab
National Aeronautics and Space Administration
Lewis Research Center

June 1979

Prepared for
U.S. DEPARTMENT OF ENERGY
Office of Conservation and Solar Applications
Division of Transportation Energy Conservation

NOTICE

DOE/NASA/1044-79/2
NASA TM-79177

PERFORMANCE OF A 14.9-kW LAMINATED-FRAME DC SERIES MOTOR WITH CHOPPER CONTROLLER

John R. Schwab
National Aeronautics and Space Administration
Lewis Research Center
Cleveland, Ohio 44135

June 1979

Prepared for
U. S. DEPARTMENT OF ENERGY
Office of Conservation and Solar Applications
Division of Transportation Energy Conservation
Washington, D. C. 20545
Under Interagency Agreement EC-77-A-31-1044

SUMMARY

Very little performance data is available for chopper controlled dc series motors as used in battery powered electric vehicles. This report presents test results obtained through experimental testing of a 14.9 kW (20 hp) traction motor using two types of excitation: ripple-free dc from a motor-generator set for baseline data and chopped dc as supplied by a battery and chopper controller. For the same average values of input voltage and current, the power output was independent of the type of excitation. However, at the same speeds, motor efficiency at low power output (corresponding to low duty cycle of the controller) was 5 to 10 percentage points less on chopped dc than on ripple-free dc. This illustrates that for chopped waveforms, it is incorrect to calculate input power as the product of average voltage and average current. Locked-rotor torque, no-load losses, and magnetic saturation data were also determined.

INTRODUCTION

Direct-current series motors with chopper controllers are used in the majority of present-day battery powered electric vehicles (ref. 1). The chopper controller is a dc to dc converter that produces a variable average output voltage from a reasonably constant voltage source. Very little performance data is available for dc motors operating under the pulse modulation voltage control provided by such controllers. Most electric vehicle manufacturers are small companies with limited capacity for testing, research, or development of propulsion system components. They are usually forced to choose a traction motor based only upon the limited data provided by the motor manufacturer for ripple-free dc operation.

The NASA Lewis Research Center has been authorized by the Department of Energy to conduct research, development, and testing of propulsion systems and components for electric and hybrid vehicles. Part of the Lewis Research Center program is focused upon characterizing existing propulsion system components. The data presented in this report is a result of the chacterization effort and will assist present-day electric vehicle manufacturers. The data will also support the development of improved components by providing a comparison baseline.

The motor that was tested and the controller have both been used in electric vehicles, although no known vehicle has used them in combination. The motor was experimentally tested under a wide range of operating conditions for two types of excitation: ripple-free dc as supplied by a motor-generator set for baseline motor data, and chopped dc as supplied by the chopper controller and battery pack. Motor efficiency and motor output power were calculated for comparison of motor performance under both types of excitation. Locked-rotor torque, no-load losses, and magnetic saturation data were also determined.

DESCRIPTION OF MOTOR AND CONTROLLER

The motor was manufactured by the Northwestern Electric Company of Chicago, Illinois, and is shown in figure 1. It is a four-pole machine with a series-parallel field winding configuration as shown in figure 2. The armature is lap wound. Rating data and dimensions are given in table 1. The motor requires forced ventilation of 0.118 m^3/s (250 ft^3/min) for its 14.9 kW (20 hp) continuous duty output power rating. Both the armature core and the stator were constructed from die-cut laminations. The commutator has 64 bars. The brushes were shifted approximately 45 electrical degrees CCW off the no-load magnetic neutral by the manufacturer. This CCW brush shift makes CW rotation the preferred direction of rotation for the motor.

The controller was manufactured by EVC, Inc., of Inglewood, California, using high current power Darlington switching transistors produced by the Semiconductor Division of EVC, Inc. Voltage control is accomplished by pulse width modulation from 0 to 100 percent duty cycle at a nominal switching rate of 400 Hz. Since duty cycle variations caused the switching rate to deviate somewhat from the nominal value, a minor modification of the controller was made at NASA to keep the switching rate constant. This change eliminated any of the effects of variable switching rate from the test results. A frequency counter was used to monitor the switching rate during the tests. The controller contains an internal flywheel diode and an input capacitor filter along with current limit, short circuit, and thermal limit protection circuits. Rating data and dimensions are given in table 2. A photograph of the controller is shown in figure 3.

APPARATUS AND PROCEDURE

A block diagram of the apparatus used in the motor testing is shown in figure 4. The drive motor was used for the no-load losses and magnetic saturation tests. An electrical connection diagram for the chopper controlled motor tests is shown in figure 5. To eliminate erratic controller operation due to battery voltage droop at high current levels, a separate 12-volt dc power supply was used to power the controller logic circuits.

Maximum values of the measurands recorded, along with their estimated accuracies, are listed in table 3. A block diagram of the instrumentation system is shown in figure 6. Coaxial shunts with extended frequency response, negligible phase shift, and very large energy capacity were used for current measurements. Wideband electronic wattmeters were used to measure electrical power. Reference 2 discusses the attributes of such instrumentation.

The motor wattmeter was used to measure the average electrical input power to the motor for both the ripple-free dc tests and the chopped dc

tests, in order to maintain consistent power measurements and to allow valid efficiency comparisons. Static and dynamic calibrations were performed on the wattmeter to check its accuracy.

Figure 7 shows the relationship of indicated power to calculated power for the static ripple-free dc calibration. Signal generators were used to provide appropriate voltage and current signals. The calculated power was computed as the product of the voltage and current signals. Figure 8 presents the correlation of the indicated power to the calculated power for the static chopped waveform calibration. For this test, the inputs consisted of 500 Hz rectangular pulse trains supplied by synchronized signal generators. The pulse train amplitudes were set equal to the full scale dc voltage and current signals. The calculated power was computed as the product of the voltage amplitude, the current amplitude, and the duty cycle. The straight line plotted on each graph represents the perfect theoretical correlation; the actual data points correspond within ±2 percent of full scale.

The results of the dynamic calibration are presented in figure 9. For this test, the inputs consisted of actual voltage and current signals during ripple-free dc operation of the motor. The calculated power was computed as the product of the average voltage and the average current. The data points lie within ±320 W of the perfect theoretical correlation line; this accuracy corresponds to ±2 percent of the 16 kW maximum power.

The scanning data logger with averaging input was used to record all measurand signals except temperature, which was visually monitored during the tests. The amplifiers in the instrumentation system were wideband floating differential types used to provide good isolation from the power circuits and high common-mode signal rejection. Oscilloscope trace photographs of the instantaneous voltage and current signals were taken at various data points.

Baseline motor performance was established by a series of ripple-free dc motor tests, powered by a large dc motor-generator set. For the chopper controlled motor tests, an 84 V battery pack consisting of 14 EV-106 lead batteries was used. The battery pack was recharged whenever the open-circuit terminal voltage dropped below 80 V, which is approximately 95 percent of the 84 V nominal open-circuit terminal voltage. This technique minimized the effects of battery state of charge on the test results.

The motor temperature was monitored by a thermocouple on one of the motor field coils. This temperature was maintained between 70 and 80° C for all performance tests by varying the warm-up loading and the cooling ventilation of the motor. An average winding temperature of 75° C was assumed for all winding resistance calculations.

For the no-load losses and magnetic saturation tests, the brushes on the motor were returned to the no-load magnetic neutral position by the reverse rotation method of the IEEE Standard Test Code for Direct-Current Machines (IEEE Std. 113-1973). The brushes were originally shifted 45 electrical degrees CCW off the no-load neutral by the manufacturer. Brush shifting changes the spatial distribution of active armature conductors to alleviate the cross-magnetizing effects of armature reaction magnetomotive force. During no-load losses and magnetic saturation tests, there is no armature current present, therefore no cross-magnetizing force exists under the prescribed test conditions. If the brushes were off the no-load magnetic neutral for these tests, the brushes would short-circuit armature conductors that were subjected to a direct-axis flux component; this condition is not representative of actual machine operation.

The motor performance tests were run with the brushes on the no-load magnetic neutral and with the brushes shifted 45 electrical degrees CCW as adjusted by the manufacturer. The CCW brush shift made the preferred direction of rotation CW; for consistency, all tests were performed with CW rotation.

The no-load losses and magnetic saturation tests were run at various speeds and various average field current levels. The motor performance tests were run by varying average motor voltage and speed to obtain several parametric matrices of data points.

RESULTS AND DISCUSSION

Performance data is presented in tables 4, 5, and 6. In table 4 the independent variables are average voltage and average current. In table 5 the independent variables are average voltage and speed. In table 6 the independent variables are average current and speed. Speed and torque were measured and motor output power was calculated in English units and then converted to SI units for the tables. The motor input power was measured by the electronic wattmeter. Figure 10 shows the output power of the motor as a function of speed, average voltage, and average current for ripple-free dc and chopped dc. The power developed by the motor at any particular speed, average voltage, and average current is virtually the same with or without the controller for both brush positions. Since the controller went into continuous conduction (100 percent duty cycle) above the 70 V level, 80 V data could not be obtained when operating with the EVC controller and the 84 V battery pack. During continuous conduction, the battery could not maintain 80 V at any of the current levels used for the remainder of the test matrix. Efficiency was calculated as the ratio of output power to input power as measured by the wattmeter. Figure 11 presents motor efficiency as a function of output power and speed. The motor appears to be approximately 5 to 10 percentage points less efficient when operated with the chopper controller at the lower power levels (corresponding to low controller duty cycle). As the power level and

the applied voltage increase, the difference between the ripple-free dc and chopped dc efficiency curves becomes smaller. The curves meet when the controller duty cycle is close to 100 percent. These results can be seen for both brush positions. The crossover of the efficiency curves should not be misinterpreted; the estimated error in the efficiency data is ±3 percent. The most significant result is that the chopped dc efficiency curve lies below the ripple-free dc efficiency curve for low to moderate power levels and low to moderate duty cycles. This suggests additional electrical or magnetic loss mechanisms in the motor during chopped dc operation, since the output power is the same for identical combinations of speed, average voltage, and average current. This also illustrates that for chopped waveforms, it is incorrect to calculate motor input power as the product of average voltage and average current.

Some typical chopped dc motor voltage and current waveforms are shown in figure 12. Because of the action of the flywheel diode, the current waveforms exhibit different time constants for build-up and decay. The reason for the different time constants is that during build-up the battery resistance is present in the circuit, while during decay, only the motor resistance is present.

Locked-rotor torque data is tabulated in table 7 and presented graphically in figure 13. Examination of table 7 and figure 13 shows that with the brushes on the no-load magnetic neutral (0^{o}), the torque developed by the motor at the same average current is independent of the type of excitation. As expected, when the brushes are shifted off the neutral to the original position as adjusted by the manufacturer (45^{o}), the torque developed is less than the torque developed when the brushes are on neutral. The unexpected result is that the chopped dc torque is greater than the ripple-free dc torque for the same average current with the brushes shifted. A possible explanation is that the ac component of the chopped current in the series field induces voltages in the armature which cause currents to flow when the brushes are not located on the neutral position. This mechanism would be similar to the operation of an ac repulsion motor.

The magnetic saturation tests yielded identical sets of constant-speed saturation curves for ripple-free dc and chopped dc excitation; these curves are shown in figure 14. Since the average armature generated voltage is the same for both types of field excitation, the average direct-axis flux in the motor is the same. The effects of armature reaction on the direct-axis flux are not included in a magnetic saturation test.

The results of the no-load losses tests are presented in tables 8 and 9 for ripple-free dc and chopped dc excitation, respectively. The mechanical losses consist of brush friction, bearing friction, and windage losses. These are functions of speed only. The I^2R losses

consist of resistive joule heating losses in the armature windings, the series field windings, and the brushes. Due to the difficulty of obtaining rms current measurements for chopped waveforms, the average value of current is used to estimate the I^2R losses. The armature and field winding resistances are calculated for the assumed constant winding temperature of 75^{o} C. The voltage drop at the brushes is reasonably approximated as 1.0 V at 50 A, 1.3 V at 100 A, 1.7 V at 150 A, and 2.0 V at 200 A. Hysteresis and eddy current losses due to changing flux densities are listed as core losses. The core losses do not include the joule heating losses in short-circuited armature windings undergoing commutation or any effects of direct-axis flux distortion due to armature reaction. Examination of tables 8 and 9 shows that the I^2R losses clearly predominate during both ripple-free dc and chopped dc operation of the motor. The chopped dc core losses are approximately equal to the ripple-free dc core losses at low current levels and approximately 5 percent greater at the high current levels.

Table 10 presents some motor efficiency data calculated from the ratio of output power to output power plus the summed losses (Method B) and data obtained from the ratio of output power to input power as measured by the wattmeter (Method A), for ripple-free dc and chopped dc operation. The summed losses used in Method B include the mechanical losses, I^2R losses, core losses, and a stray load loss calculated as the standard one percent of the output as prescribed in IEEE Std. 113-1973. Examination of the results shows that the Method B efficiencies do not match the Method A efficiencies for either ripple-free or chopped dc excitation. This suggests that the standard stray load loss calculation is not sufficient for precise determination of motor efficiency. Further examination of table 10 shows that there is almost no change in efficiency between ripple-free dc and chopped dc operation when the summed-losses calculation (Method B) is used. If the Method A efficiency calculation is assumed to be correct, these results suggest that the standard stray load loss calculation is especially not applicable when the motor is operated with a chopper controller. Additional electrical or magnetic loss mechanisms may occur due to the chopped voltage and current waveforms in the motor, especially at low average voltage levels when the crest factor (peak to average ratio) of the voltage waveform is very high. Some possible loss mechanisms that may be present for chopped dc operation are:

1. Increased effective impedance due to non-uniform current distribution (skin effect and proximity effect) caused by the ac components of the current.

2. Additional I^2R losses at the same average current level due to the rms content of the ac current components.

3. Increased commutation losses caused by higher induced voltages in short-circuited armature windings undergoing commutation.

4. Increased brush voltage drop due to ac components in the armature current.

5. Poor commutation due to ac components in the armature current.

6. Eddy-current and hysteresis losses in the stator frame and poles due to chopped current waveform.

7. Increased direct-axis flux distortion under load due to armature reaction magnetomotive force created by chopped armature current.

8. Additional magnetic reluctance and airgap flux distortion due to varying permeability of magnetic circuit (especially the pole faces) under varying flux conditions.

SUMMARY OF RESULTS

The Northwestern motor was tested to determine its performance when operated with the EVC chopper controller and a battery pack. Baseline ripple-free dc performance data was obtained by exciting the motor from a variable-voltage motor-generator set. No-load losses and magnetic saturation data were also determined for ripple-free dc and chopped dc operation of the motor. All performance tests were run for two brush positions: the original position, as adjusted by the manufacturer, and the no-load magnetic neutral position. The no-load losses and saturation tests were performed for the neutral position only.

The motor was 5 to 10 percentage points less efficient on chopped dc than on ripple-free dc at low output power levels at the same speeds. At higher output power levels, as the controller duty cycle approached 100 percent, the chopped dc efficiency approached the ripple-free dc efficiency. The output power developed for the same average voltage and average current was virtually identical for both ripple-free dc and chopped dc operation. These results were observed for both brush positions. The locked-rotor torque tests showed equal torque developed at same average current for ripple-free dc and chopped dc excitation with the brushes on neutral. With the brushes shifted off neutral to the original position, the chopped dc torque was greater than the ripple-free torque for the same average current. The magnetic saturation curves were identical for both types of field excitation. At low average current levels, the core losses were approximately the same for both types of excitation. At higher average current levels, the chopped dc core losses were approximately 5 percent greater than the ripple-free dc core losses. Efficiency calculations by the summed losses method with the standard stray load loss assumption yielded poor correlation with the efficiency calculations using the ratio of output power to measured input power.

REFERENCES

1. State-of-the-Art Assessment of Electric and Hybrid Vehicles. CONS/1011-1, NASA TM-73756, 1977.

2. Triner, James E.; and Hansen, Irving G.: Electric Vehicle Power Train Instrumentation - Some Constraints and Considerations. ERDA/NASA-1011/77/1, NASA TM X-73629, 1977.

Table 1. - Motor Data

Manufacturer	Northwestern Electric Company
Model number	250-100-0033 A
Serial number	20631-DB
Rated continuous output power, kW (hp)	14.9 (20)
Rated dc voltage, V	84
Rated dc current, A	210
Rated shaft speed, rad/s (rpm)	419 (4000)
Insulation class	F
Maximum ambient temperature, ^{o}C	40
Average airgap length, mm (in.)	1.02 (0.040)
Stator outside diameter, m (in.)	0.31 (12.25)
Overall frame diameter, m (in.)	0.36 (14.0)
Overall frame length, m (in.)	0.46 (18.1)
Mass, kg (lbm)	84.8 (187)
Armature winding resistance at 25^{o} C, ohms	0.011
Series field winding resistance at $25^{o}C$, ohms	0.008
Preferred direction of rotation, viewed from anti-drive end	CW

Table 2. - Controller Data

Manufacturer	EVC, Inc.
Model number	400-96-12-H
Serial number	1405
Maximum input voltage, V	96
Maximum output current, A	400
Overall length, m (in.)	0.26 (10.25)
Overall width, m (in.)	0.18 (7.25)
Overall depth, m (in.)	0.10 (4.0)
Mass, kg (lbm)	5.7 (12.5)

Table 3. - Measurands and Accuracies

Measurand	Full-scale calibration	Accuracy % full scale
Average input voltage	100 V	±0.5
Average input current	250 A	±0.5
Average input power	16 kW	±2.0
Average motor voltage	100 V	±0.5
Average motor current	250 A	±0.5
Average motor power	16 kW	±2.0
Shaft speed	524 rad/s (5000 rpm)	±0.2
Shaft torque	108.5 N-m (80.0 lbf-ft)	±0.5
Motor temperature	100° C	±2.0

Table 4. - Motor Performance Data With Average Voltage and Average Current as Independent Variables

Ripple-free dc, brushes on neutral

Avg. voltage V	Avg. current A	Motor input power W	Torque N-m	Speed rad/s	Motor output power W	Efficiency %
20.0	52.9	1087	6.8	114	772	71.0
20.1	101.0	2107	18.7	81	1512	71.8
20.0	152.3	3127	31.4	66	2072	66.3
20.0	203.6	4265	46.0	55	2529	59.3
39.9	51.3	1832	6.4	238	1515	82.7
39.9	101.0	3912	18.6	179	3327	85.0
39.9	152.3	6070	31.4	155	4869	80.2
40.0	202.0	8149	45.0	139	6251	76.7
59.9	51.3	2656	5.7	354	2016	75.9
60.0	102.6	5874	18.2	273	4966	84.5
60.0	150.7	8934	31.0	240	7450	83.3
59.9	203.6	12190	44.6	218	9717	79.7
79.8	102.6	7796	17.9	368	6584	84.5
79.9	152.3	11955	30.8	324	9963	83.3
79.8	202.0	16153	43.5	295	12840	79.4

Table 4. - Continued

Chopped dc (400 Hz), brushes on neutral

Avg. voltage V	Avg. current A	Motor input tower W	Torque N-m	Speed rad/s	Motor output power W	Efficiency %
20.0	52.9	1479	6.4	117	747	50.5
19.9	99.4	2539	17.2	84	1445	56.9
19.7	147.5	3519	30.0	68	2040	58.0
20.2	200.4	4500	45.7	58	2652	58.9
40.1	52.9	2499	6.8	238	1614	64.6
39.9	101.0	4422	17.9	181	3245	73.4
39.9	152.3	6462	30.4	157	4768	73.8
39.7	202.0	8502	44.9	139	6237	73.4
59.9	52.9	2970	6.4	354	2256	76.0
59.9	102.6	5913	17.9	275	4926	83.3
59.6	152.3	9012	30.7	240	7375	81.8
59.9	200.4	11955	44.6	217	9675	80.9

Table 4. - Continued

Ripple-free dc, brushes shifted 45°

Avg. voltage V	Avg. current A	Motor input power W	Torque N-m	Speed rad/s	Motor output power W	Efficiency %
20.3	52.9	1162	5.2	144	738	63.5
20.2	104.2	2287	16.3	93	1513	66.2
20.2	150.7	3291	27.8	75	2093	63.6
19.7	203.6	4296	41.1	63	2577	60.0
40.1	52.9	1845	4.7	311	1474	79.9
39.8	102.6	3934	15.3	217	3318	84.3
39.7	152.3	5983	27.1	183	4942	82.6
39.7	203.6	8192	40.4	162	6546	79.9
59.9	102.6	5742	14.9	346	5144	89.6
59.7	152.3	8915	26.4	295	7767	87.1
59.7	202.0	12089	38.6	264	10182	84.2
79.8	153.9	12089	26.8	398	10664	88.2
79.7	202.0	16066	39.3	361	14153	88.1

Table 4. - Concluded

Chopped dc (400 Hz), brushes shifted 45°

Avg. voltage V	Avg. current A	Motor input power W	Torque N-m	Speed rad/s	Motor output power W	Efficiency %
20.3	54.5	1684	5.2	153	786	46.7
19.6	105.8	2809	15.6	97	1504	53.5
20.2	152.3	3773	26.4	83	2176	57.7
20.9	205.2	4938	41.8	71	2961	59.9
40.8	54.5	2568	5.4	328	1776	69.2
40.0	102.6	4617	15.3	222	3391	73.4
39.7	150.7	6465	26.2	185	4834	74.8
39.7	203.6	8674	40.7	161	6514	75.0
61.0	104.2	5983	14.6	356	5202	86.9
59.6	150.7	8875	25.8	294	7552	85.1
59.9	203.6	12009	39.3	263	10311	85.9

Table 5. - Motor Performance Data With Average Voltage and Speed As Independent Variables

Ripple-free dc, brushes on neutral

Avg. voltage V	Avg. current A	Motor input power W	Torque N-m	Speed rad/s	Motor output power W	Efficiency %
20.0	222.8	4775	51.1	53	2707	56.7
19.8	59.3	1322	8.2	105	856	64.8
20.0	22.4	538	0.7	209	142	26.4
40.0	68.9	2735	10.2	210	2132	78.0
59.8	219.6	13406	49.3	210	10348	77.2
40.0	35.3	1322	2.3	314	724	54.8
60.0	72.1	4069	10.4	314	3281	80.6
79.9	166.7	13328	34.5	314	10824	81.2
59.9	41.7	2107	3.0	419	1250	59.3
79.8	73.7	5403	10.4	419	4374	81.0

Table 5. - Continued

Chopped dc (400 Hz), brushes on neutral

Avg. voltage V	Avg. current A	Motor input power W	Torque N-m	Speed rad/s	Motor output power W	Efficiency %
10.0	52.9	1087	6.1	56	341	31.4
20.0	67.3	1832	9.2	105	968	52.8
19.7	22.4	852	0.7	209	142	16.7
40.6	75.3	3323	11.3	209	2356	70.9
40.4	33.7	1597	2.4	314	767	48.0
59.8	73.7	4343	10.6	314	3321	76.5
39.7	22.4	1126	0.4	417	170	15.1
60.0	41.7	2421	3.4	419	1420	58.7

Table 5. - Continued

Ripple-free dc, brushes shifted 45°

Avg. voltage V	Avg. current A	Motor input power W	Torque N-m	Speed rad/s	Motor output power W	Efficiency %
19.9	86.6	1845	12.6	105	1323	71.7
20.0	36.9	801	1.8	211	370	46.2
40.2	117.0	4537	18.3	210	3838	84.6
39.8	56.1	1925	5.2	315	1619	84.1
60.0	126.6	7309	20.3	315	6392	87.5
39.9	36.9	1122	1.8	420	739	65.9
59.7	68.9	3492	7.5	420	3126	89.5
80.0	131.4	9839	21.4	420	8981	91.3

Table 5 - Concluded

Chopped dc (400 Hz), brushes shifted 45°

Avg. voltage V	Avg. current A	Motor input power W	Torque N-m	Speed rad/s	Motor output power W	Efficiency %
10.0	75.3	1363	8.8	53	462	33.9
10.0	33.7	841	1.4	105	142	16.9
20.3	104.2	2608	14.6	105	1532	58.7
20.1	38.5	1122	2.0	211	427	38.1
39.9	123.4	5099	18.3	210	3832	75.2
41.0	59.3	2528	5.8	315	1832	72.5
59.7	136.2	7830	21.0	315	6599	84.3
40.4	38.4	1644	2.4	421	1025	62.3
60.0	72.1	3854	7.9	420	3292	85.4

Table 6. - Motor Performance Data With Average Current And Speed As Independent Variables

Ripple-free dc, brushes on neutral

Avg. voltage V	Avg. current A	Motor input power W	Torque N-m	Speed rad/s	Motor output power W	Efficiency %
10.0	52.9	930	6.3	53	336	36.1
13.9	101.0	1754	18.3	52	951	54.2
16.8	152.3	2853	31.3	53	1657	58.1
19.0	202.0	4226	45.0	53	2386	56.5
18.5	51.3	1205	6.1	105	640	53.1
24.7	102.6	2735	18.1	105	1901	69.5
28.4	152.3	4618	31.4	105	3301	71.5
31.5	202.0	6658	44.9	105	4710	70.7
34.2	51.3	1872	5.7	210	1194	63.8
45.9	101.0	4697	17.9	210	3753	79.9
52.8	152.3	8188	31.4	210	6595	80.5
57.8	202.0	11916	44.5	210	9353	78.5
52.9	52.9	2578	6.1	314	1916	74.3
68.6	102.6	6854	17.9	314	5625	82.1
77.7	150.7	11680	30.4	314	9536	81.6
68.6	52.9	3206	5.4	419	2274	70.9

Table 6. - Continued

Chopped dc (400 Hz), brushes on neutral

Avg. voltage V	Avg. current A	Motor input power W	Torque N-m	Speed rad/s	Motor output power W	Efficiency %
9.5	52.9	1087	6.1	52	318	29.3
13.5	102.6	2068	17.8	52	923	44.6
16.4	152.3	3088	32.1	52	1669	54.0
18.8	202.0	4226	46.5	53	2464	58.3
17.7	52.9	1440	6.1	105	642	44.6
23.9	102.6	2931	17.3	105	1821	62.1
27.6	150.7	4618	29.7	105	3121	67.6
31.0	202.0	6737	45.4	105	4767	70.8
34.0	52.9	2186	6.1	209	1277	58.4
45.4	104.2	4893	18.1	209	3775	77.2
51.6	152.3	7914	29.9	209	6245	78.9
57.0	202.0	11641	45.3	209	9467	81.3
51.2	51.3	2813	5.8	314	1832	65.1
66.8	102.6	6501	16.9	314	5321	81.8
67.7	52.9	3245	5.8	419	2442	75.3

Table 6. - Continued

Ripple-free dc, brushes shifted 45°

Avg. voltage V	Avg. current A	Motor input power W	Torque N-m	Speed rad/s	Motor output power W	Efficiency %
8.5	52.9	720	5.2	53	271	37.6
12.9	102.6	1524	16.7	53	884	58.0
15.5	152.3	2568	28.9	53	1521	59.2
17.7	200.4	3773	41.1	53	2151	57.0
14.6	51.3	921	5.2	105	540	58.6
21.6	102.6	2367	16.3	105	1707	72.1
25.4	150.7	3974	27.8	105	2908	73.2
28.4	202.0	5902	41.1	105	4311	73.0
25.7	51.3	1283	4.5	209	935	72.9
38.1	104.2	3813	15.3	210	3208	84.1
44.8	152.3	6786	27.1	210	5686	83.6
49.1	200.4	9839	39.1	210	8175	83.1
38.0	51.3	1684	4.1	315	1277	75.8
54.8	102.6	5259	14.9	315	4683	89.0
64.0	150.7	9438	26.4	315	8301	87.9
70.0	202.0	14299	39.1	315	12273	85.8
51.4	52.9	2207	4.5	420	1873	84.9
73.0	101.0	6947	14.9	420	6253	90.0
84.7	150.7	12571	26.8	420	11246	89.5

Table 6. - Concluded

Chopped dc (400 Hz), brushes shifted 45°

Avg. voltage V	Avg. current A	Motor input power W	Torque N-m	Speed rad/s	Motor output power W	Efficiency %
7.8	52.9	1001	4.5	53	237	23.7
12.1	104.2	1885	14.9	53	786	41.7
15.1	152.3	2729	25.4	53	1330	48.7
17.0	205.2	3974	40.7	53	2156	54.3
13.7	52.9	1202	4.5	105	467	38.9
20.3	104.2	2608	14.6	105	1532	58.7
24.2	150.7	4095	25.5	106	2683	65.5
27.4	203.6	5943	39.3	105	4114	69.2
25.8	54.5	1724	4.5	210	937	54.4
37.0	102.6	4095	14.2	211	2989	73.0
43.6	153.9	6706	25.5	210	5345	79.7
48.4	200.4	9839	38.0	210	7960	80.9
37.4	52.9	2126	4.5	315	1406	66.1
53.7	104.2	5340	14.2	314	4466	83.6
63.0	152.3	9116	25.1	315	7884	86.5
50.6	54.5	2568	4.7	420	1988	77.4

Table 7. - Locked-Rotor Torque

Brushes on neutral

Avg. current A	Ripple-free dc torque N-m	Chopped dc torque N-m
50.0	6.8	6.5
100.0	20.1	20.1
150.0	33.2	33.6
200.0	47.5	47.2
250.0	61.7	61.0

Brushes shifted 45°

Avg. current A	Ripple-free dc torque N-m	Chopped dc torque N-m
50.0	6.4	6.4
100.0	18.0	19.3
150.0	30.2	31.9
200.0	42.0	44.1
250.0	54.6	57.3

Table 8. - Ripple-free dc No-load Losses, Brushes on Neutral

Speed rad/s (rpm)	Average current A	Mechanical losses W	I^2R losses W	Core losses W
52 (500)	50	62	108	9
	100	62	360	20
	150	62	773	25
	200	62	1320	29
105 (1000)	50	128	108	28
	100	128	360	53
	150	128	773	67
	200	128	1320	81
209 (2000)	50	270	108	71
	100	270	360	142
	150	270	773	184
	200	270	1320	220
314 (3000)	50	426	108	118
	100	426	360	235
	150	426	773	299
	200	426	1320	363
419 (4000)	50	682	108	199
	100	682	360	384
	150	682	773	483
	200	682	1320	597

Table 9. - Chopped dc No-load Losses, Brushes on Neutral

Speed rad/s (rpm)	Average current A	Mechanical losses W	I^2R losses W	Core losses W
52 (500)	50	62	108	11
	100	62	360	20
	150	62	773	25
	200	62	1320	31
105 (1000)	50	128	108	28
	100	128	360	53
	150	128	773	71
	200	128	1320	81
209 (2000)	50	270	108	71
	100	270	360	142
	150	270	773	191
	200	270	1320	220
314 (3000)	50	426	108	128
	100	426	360	245
	150	426	773	320
	200	426	1320	394
419 (4000)	50	682	108	199
	100	682	360	384
	150	682	773	511
	200	682	1320	639

Table 10. - Efficiency Comparisons

Ripple-free dc, brushes on neutral

Avg. voltage V	Avg. current A	Speed rad/s (rpm)	Output power W	Efficiency, Method A[1] %	Efficiency, Method B[2] %
14	100	52 (500)	951	54.2	67.8
19	200	52 (500)	2386	56.5	62.4
46	100	209 (2000)	3753	79.9	82.2
58	200	209 (2000)	9353	78.5	83.1
69	50	419 (2000)	2274	70.9	69.2

Chopped dc (400 Hz), brushes on neutral

14	100	52 (500)	923	44.6	67.2
19	200	52 (500)	2464	58.3	63.1
45	100	209 (2000)	3775	77.2	82.3
57	200	209 (2000)	9467	81.3	82.5
68	50	419 (4000)	2442	75.3	70.7

[1]Method A: Efficiency = (Output Power)/(Input Power).

[2]Method B: Efficiency = (Output Power)/(Output Power + Summed Losses).

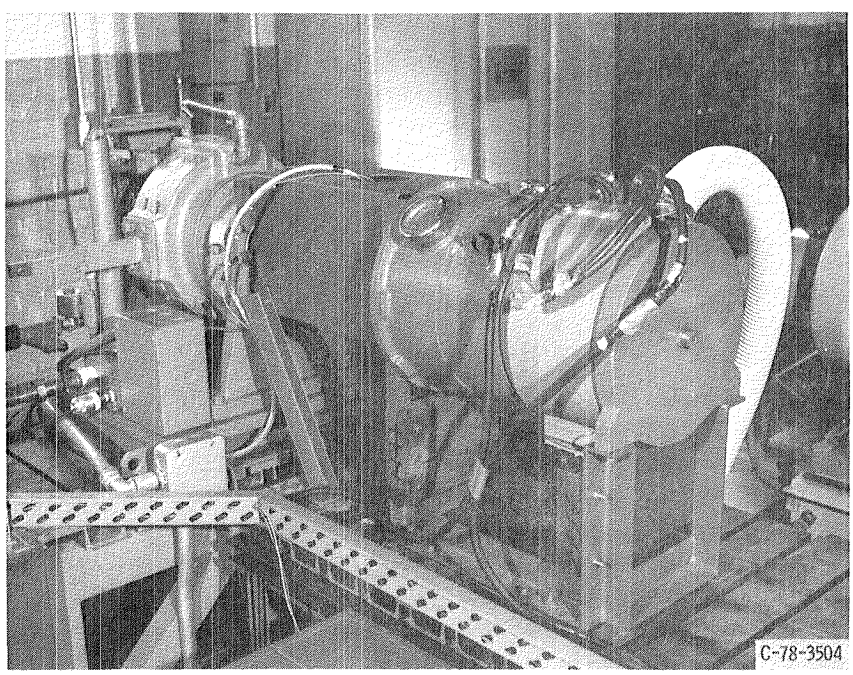

Figure 1. - Northwestern motor mounted on test stand.

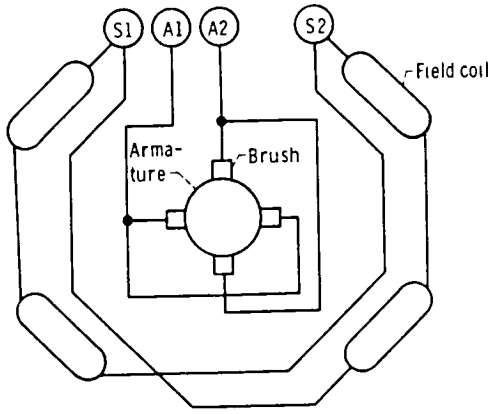

Figure 2 - Northwestern motor schematic

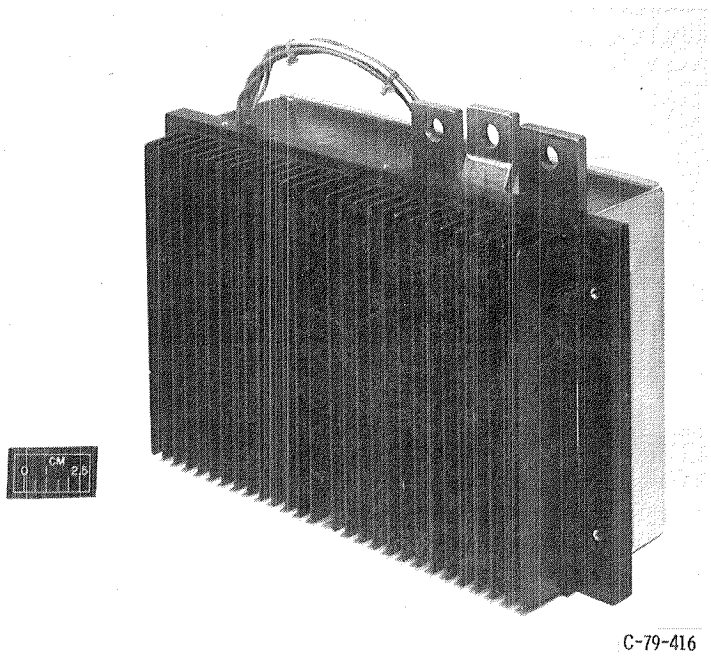

C-79-416

Figure 3. - EVC controller.

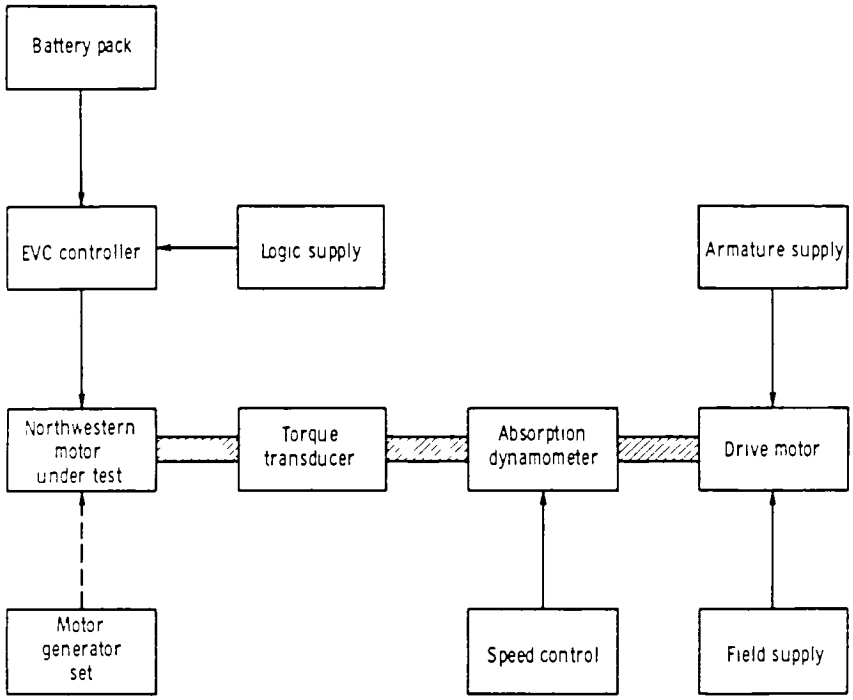

Figure 4 - Test apparatus

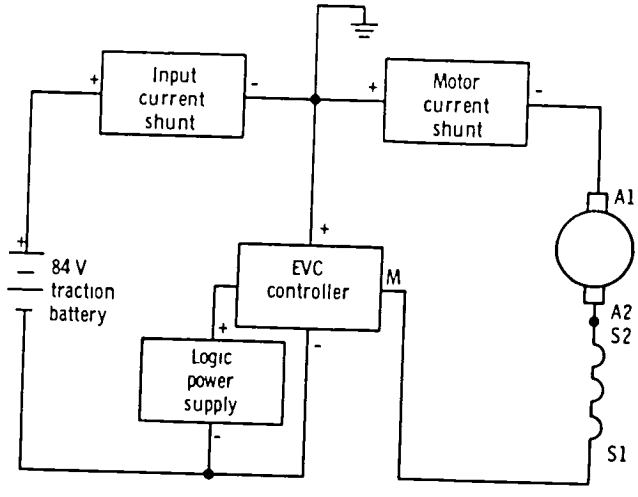

Figure 5 - Test electrical connection diagram

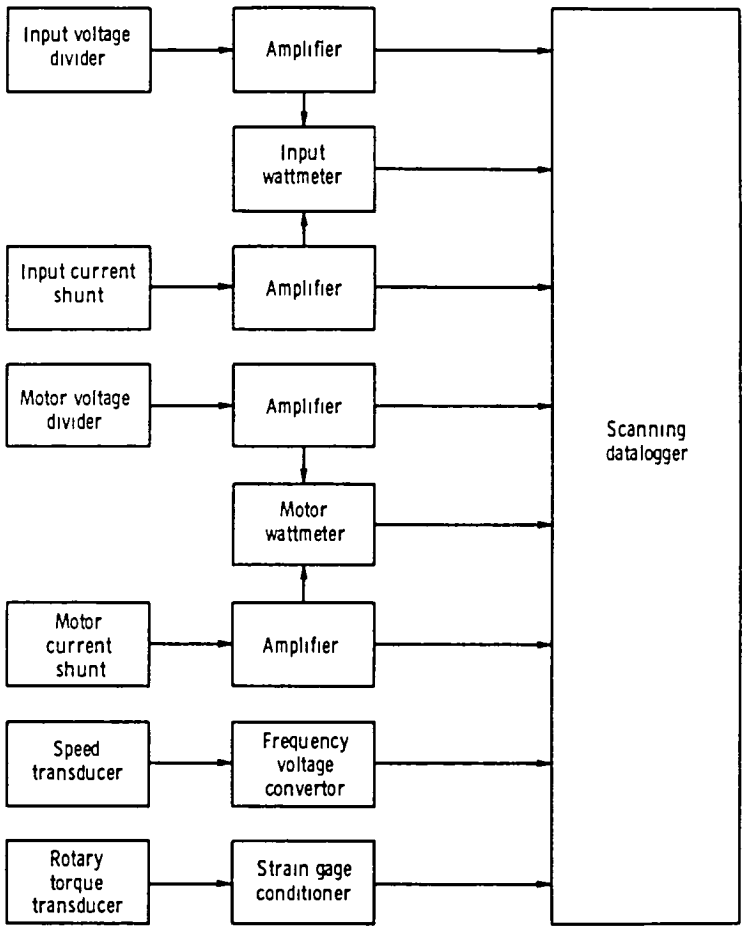

Figure 6 - Instrumentation system

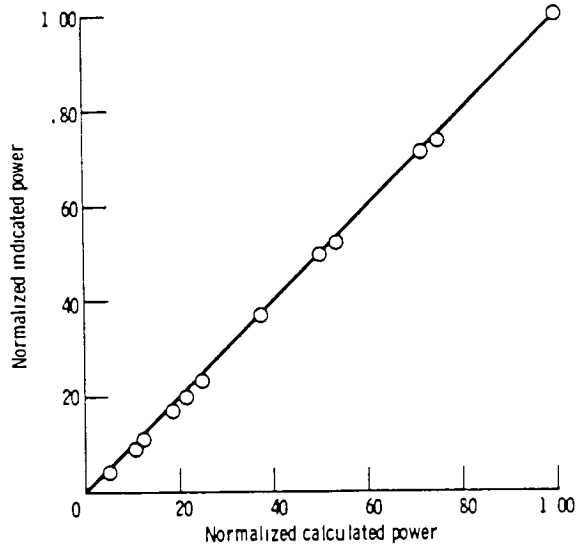

Figure 7 - Correlation of electronic wattmeter measurements with calculated power for ripple-free dc signals

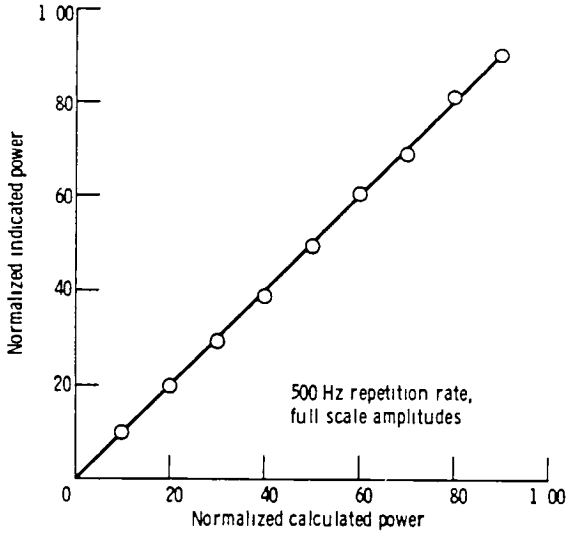

Figure 8 - Correlation of electronic wattmeter measurements with calculated power for rectangular pulse train signals

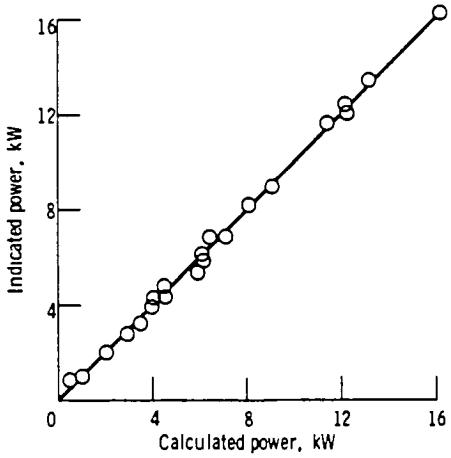

Figure 9 - Correlation of electronic wattmeter measurements with calculated power for ripple-free dc motor operation

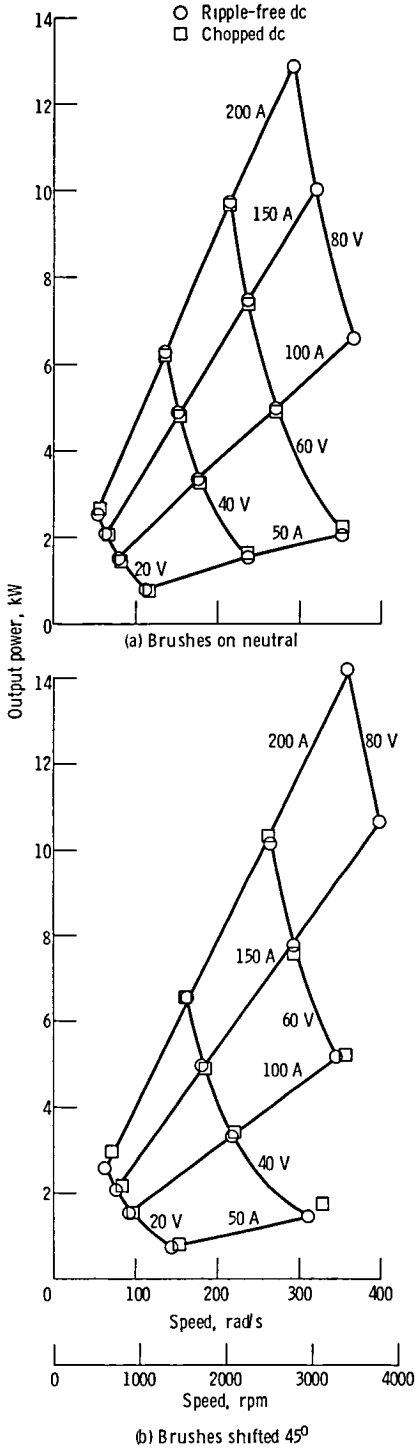

Figure 10 - Comparison of motor output power for ripple-free dc and chopped dc operation

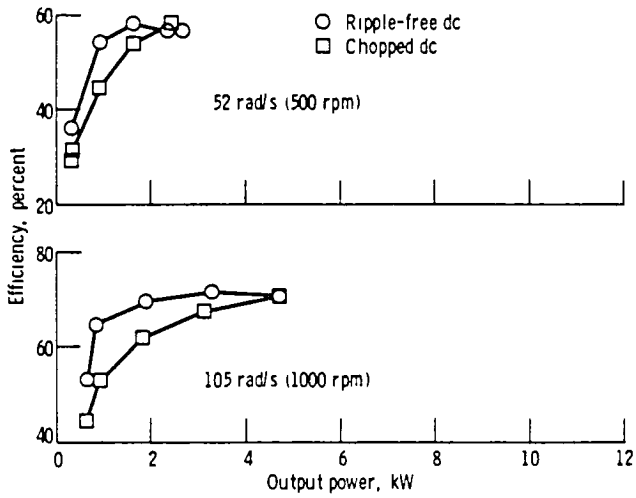

(a) Brushes on neutral.

Figure 11 - Motor efficiency at constant speed

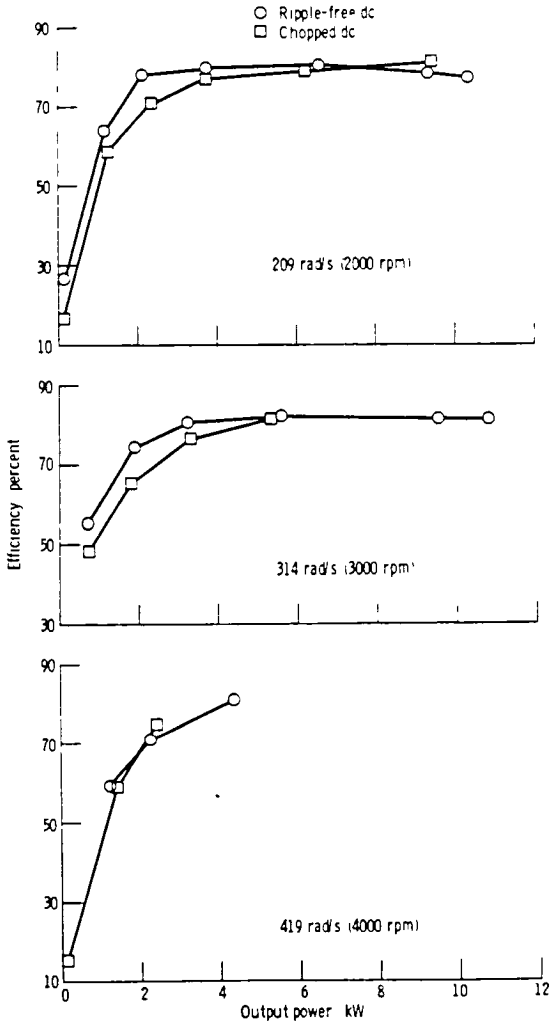

(a) Concluded

Figure 11 - Continued

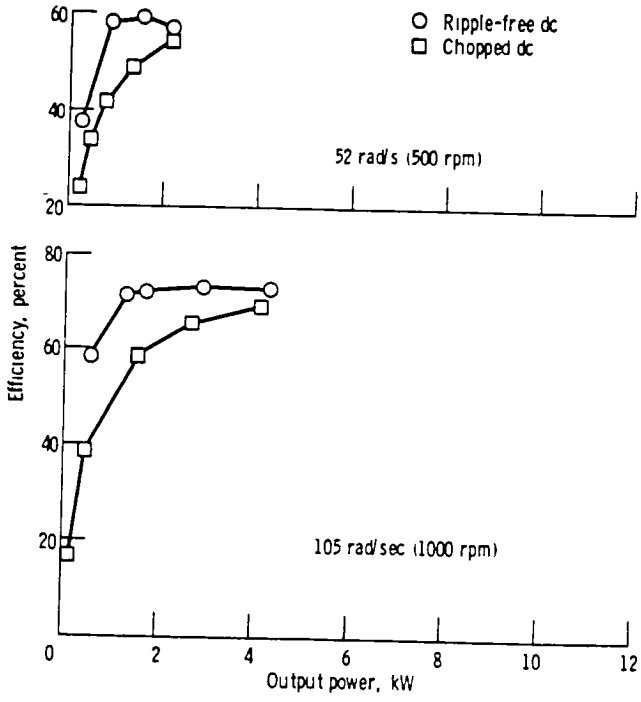

(b) Brushes shifted 45°

Figure 11 - Continued

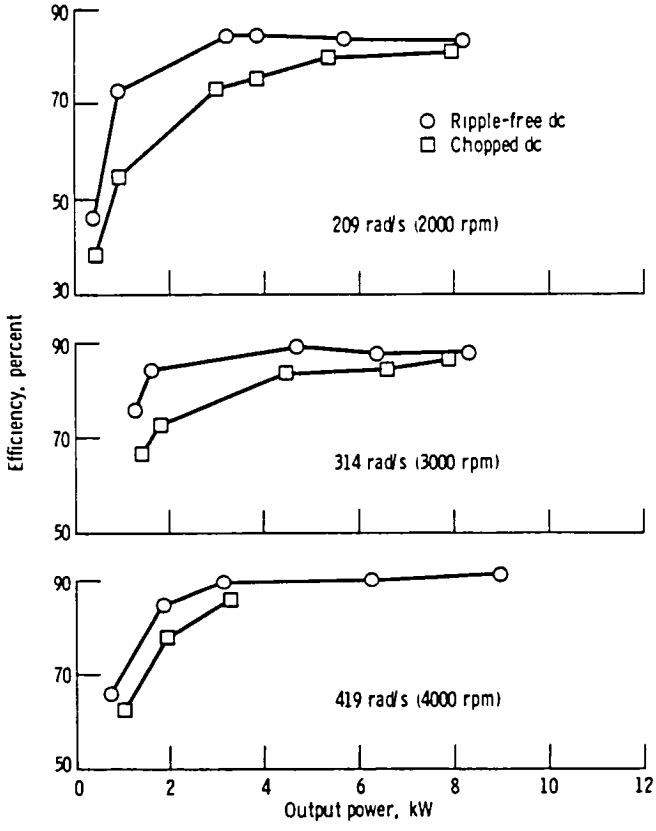

(b) Concluded

Figure 11 - Concluded

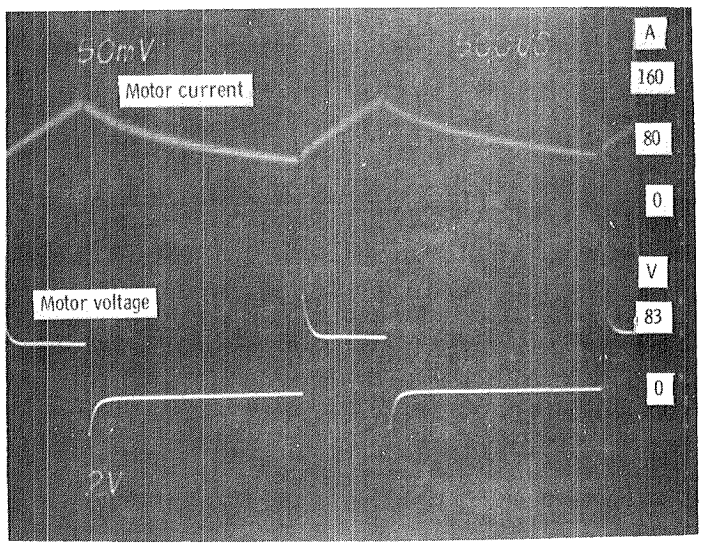

Average current, 100 A; average voltage, 20 V.

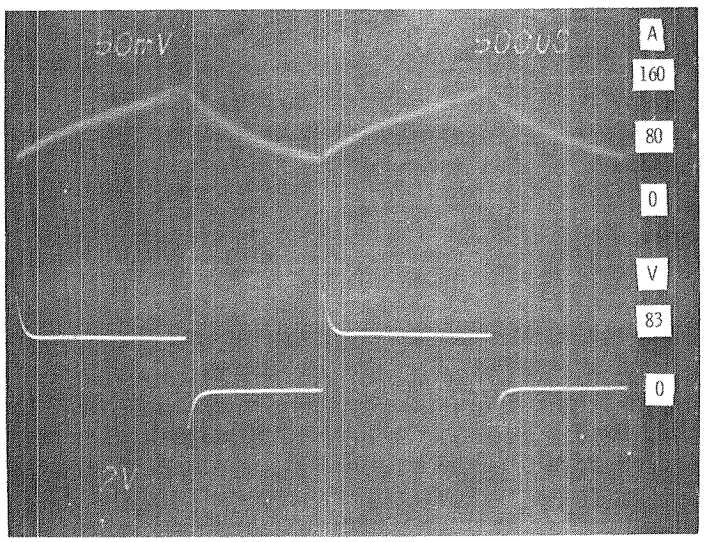

Average current, 100 A; average voltage, 40 V.

Figure 12. - Typical voltage and current waveforms with pulse width modulated controller.

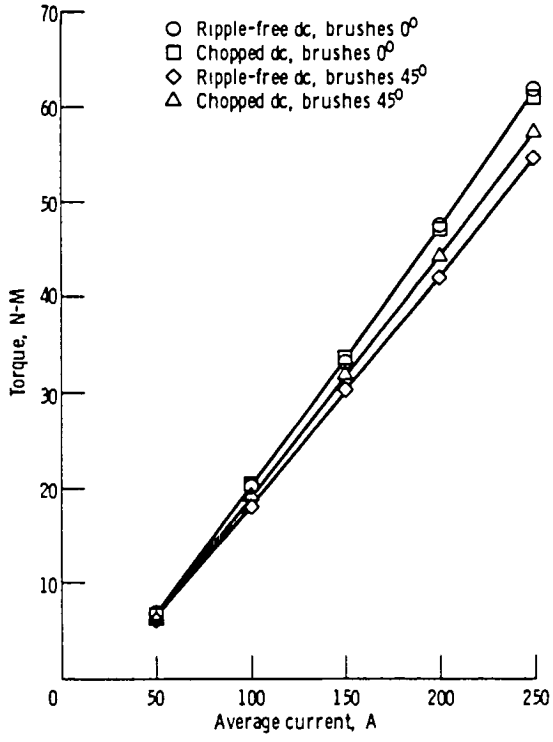

Figure 13 - Locked-rotor torque

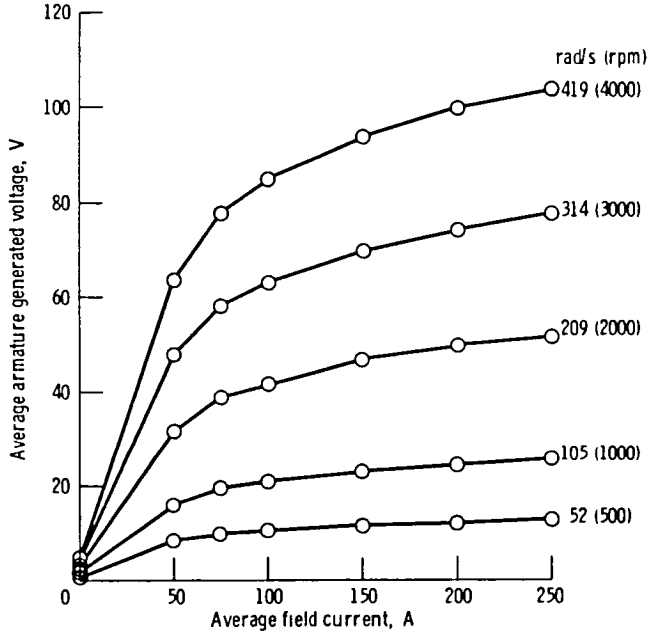

Figure 14 - Magnetic saturation curves at constant speed with brushes on neutral

1 Report No	2 Government Accession No	3 Recipient's Catalog No
NASA TM-79177		

4 Title and Subtitle	5 Report Date
PERFORMANCE OF A 14 9-kW LAMINATED-FRAME DC SERIES MOTOR WITH CHOPPER CONTROLLER	6 Performing Organization Code

7 Author(s)	8 Performing Organization Report No
John R Schwab	E-044
	10 Work Unit No

9 Performing Organization Name and Address	11 Contract or Grant No
National Aeronautics and Space Administration Lewis Research Center Cleveland, Ohio 44135	13 Type of Report and Period Covered Technical Memorandum

12 Sponsoring Agency Name and Address	14 Sponsoring Agency ~~Code~~ Report No
U.S Department of Energy Division of Transportation Energy Conservation Washington, D C 20545	DOE/NASA/1044-79/2

15 Supplementary Notes

Final report Prepared under Interagency Agreement EC-77-A-31-1044

16 Abstract

Very little performance data is available for chopper controlled dc series motors as used in battery powered electric vehicles This report presents test results obtained through experimental testing of a 14.9 kW (20 hp) traction motor using two types of excitation ripple-free dc from a motor generator set for baseline data and chopped dc as supplied by a battery and chopper controller For the same average values of input voltage and current, the power output was independent of the type of excitation. However, at the same speeds, motor efficiency at low power output (corresponding to low duty cycle of the controller) was 5 to 10 percentage points less on chopped dc than on ripple-free dc. This illustrates that for chopped waveforms, it is incorrect to calculate input power as the product of average voltage and average current Locked-rotor torque, no-load losses, and magnetic saturation data were also determined

17 Key Words (Suggested by Author(s))	18 Distribution Statement
Electric vehicles Electric motors	Unclassified - unlimited STAR Category 33 DOE Category UC-96

19 Security Classif (of this report)	20 Security Classif (of this page)	21 No of Pages	22 Price*
Unclassified	Unclassified		

* For sale by the National Technical Information Service, Springfield Virginia 22161

End of Document